Comparison of Magnetic Materials for V-Groove Inductors and MOSFETs in Optimised High-Frequency DC-DC Converters

P. Dhagat
S. Prabhakaran
C. R. Sullivan

From *IEEE Transactions on Magnetics,* vol. 40, no. 4, pp. 2008–2010.

Comparison of Magnetic Materials for V-Groove Inductors in Optimized High-Frequency DC-DC Converters

Parul Dhagat, *Student Member, IEEE*, Satish Prabhakaran, *Student Member, IEEE*, and Charles R. Sullivan, *Member, IEEE*

***Abstract*—The tradeoff between saturation flux density and resistivity in soft magnetic materials for thin film inductors is examined quantitatively. We use an optimization routine to evaluate the achievable efficiency and power density using designs individually optimized to make best use of particular materials. The optimization selects switching frequency, ripple ratio, inductor dimensions and MOSFET sizes. For the example application of a 3.3- to 1.1-V, 7-A output dc-to-dc converter, Co-Zr-O, Fe-Al-O and Co-Fe-B-Si-O materials are considered. Predicted efficiencies are in the range of 80% to 90% at power densities of 20 W/cm^2 to 1000 W/cm^2. Different materials show advantages in different power-density or efficiency ranges.**

***Index Terms*—Co-Fe-B-Si-O, Co-Zr-O, DC-DC converters, Fe-Al-O, granular films, high frequency, inductors, optimization, soft magnetic materials.**

I. Introduction

FOR soft magnetic materials used in thin-film inductors for microfabricated dc-to-dc converters, both high saturation flux density (M_s) and high resistivity are important. In developing soft magnetic materials, there is often a tradeoff between these two parameters [1]. In order to guide selection of materials and development of new materials, it is necessary to quantitatively assess the effect of the parameters on performance in the application. Although it would be simple to assess the impact of changing M_s and resistivity in a particular inductor design, that would overlook the possibility of redesigning the inductor to take best advantage of the new material.

In order to compare the possible performance of thin-film inductors using different materials, we use an optimization routine to choose inductor and dc-to-dc converter circuit parameters to get the best possible performance with each material. The converter includes an inductor, two MOSFETs and capacitors. We evaluate performance in terms of efficiency and power density (output power per unit area of substrate, including the area of the MOSFETs and the inductor), for the example of a buck converter. The results include optimized designs for the inductor and the MOSFETs.

The inductor design we consider is a V-groove inductor [2]–[4] which is in the form of a triangular wire surrounded by magnetic material, embedded in a silicon substrate as shown in Fig. 1. The fabrication process for these devices can be summarized as follows; more details are provided in [3]. A V-trench is formed by anisotropic etching of a silicon substrate. Composite magnetic material, for example Co-ZrO$_2$, is deposited in the trench to form the core. Copper is filled in the groove to form the conductor and an overlayer of magnetic material completes the core of the inductor. The magnetic material is wrapped around a single wire, thus forming a one-turn inductor.

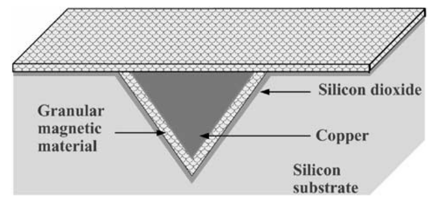

Fig. 1. Schematic of V-groove inductor (not to scale).

Section II describes the optimization routine and in Section III we investigate the performance of a 3.3- to 1.1-V, 7-A output, buck converter when different core materials are used for the V-groove inductor.

II. Design

This section explains the optimization of the inductor and MOSFETs for maximum output power per unit substrate area for any given efficiency. We start by equating the inductance requirement (L) for the dc-to-dc converter to the contribution of inductance due to the magnetic core

$$\frac{V_{\text{out}}\left(1-\frac{V_{\text{out}}}{V_{\text{in}}}\right)}{r_R I_{\text{out}} f} = \frac{N^2\mu_o\mu_r t l_L}{\left(\frac{\mu_o\mu_r N I_{\text{out}}\left(1+\frac{r_R}{2}\right)}{B_{\text{peak}}}\right)} \qquad (1)$$

where r_R is the ripple ratio (the ratio of the peak to peak amplitude of triangular inductor current waveform), f is the switching frequency of the converter, μ_o is the permeability of free space, μ_r is the relative permeability of the magnetic core, t is the thickness of the core, l_L is the length of the device and B_{peak} is peak operating flux density. The analysis is detailed in [2]. We assume that the thickness of the core is fixed at 10 μm by practical constraints. The length of the device can be calculated given ripple ratio and frequency. A large ripple ratio and a large frequency might seem to be rewarding choices for maximizing power density but could lead to high losses in both the inductor and the MOSFETs. The optimization routine evaluates this tradeoff to find the right choice of ripple ratio and frequency.

Manuscript received October 15, 2003. This work was supported in part by the Intel Corporation and in part by the National Science Foundation (NSF) under Grant ECS-9875204.

The authors are with the Thayer School of Engineering, Dartmouth College, Hanover, NH 03755 USA (e-mail: parul.dhagat@dartmouth.edu; satish.prabhakaran@dartmouth.edu; chrs@dartmouth.edu).

Digital Object Identifier 10.1109/TMAG.2004.832480

TABLE I
DESIGN PARAMETERS FOR BUCK CONVERTER

Converter specifications 3.3 V to 1.1 V, 7 A dc-to-dc converter			
Inductor geometry constraint: core thickness 10 μm			
Reference MOSFET parameters based on 0.13 μ, 3.3 V CMOS process with 33 Å gate oxide and 200 Ω/sq channel parasitic resistance			
	Area (μm^2)	R_{dson} (mΩ)	E_{switch} (fJ)
NMOS	0.78	5.10	2970
PMOS	0.78	14.72	3135
The reference parameters are scaled as described in the text to get the optimum size MOSFETs			

TABLE II
PROPERTIES OF Co-Zr-O GRANULAR FILMS [8]

$No.$	$Composition$	$B_s\ (T)$	$H_c\ (Oe)$	ρ ($\mu\Omega$-cm)	μ_r
1	$Co_{57.5}Zr_{12.5}O_{30}$	0.9	3	2000	72
2	$Co_{64}Zr_{10}O_{26}$	1.0	1	600	83
3	$Co_{63.5}Zr_{10}O_{26.5}$	1.0	3.5	750	67
4	$Co_{53.3}Zr_{11.5}O_{35}$	0.7	3	10000	70

The losses associated with the inductor and the MOSFETs must be calculated. The conductor losses are calculated from the dc resistance and the ac resistance; the ac resistance is calculated at each frequency in a Fourier series representation of the current waveform [2]. The core eddy-current loss is also calculated using a Fourier series representation of the ac flux waveform. Hysteresis loss is not calculated using Fourier analysis since it is insensitive to frequency and is nonlinear; it is estimated from coercivity and ac flux amplitude as described in [2].

To optimize the switches, we start with a reference MOSFET $(M_{\rm ref})$ with a channel area $A_{\rm ref}$ using a 0.13 μm, 3.3 V technology model derived from [5], [6]. The optimum size is given by $A_{\rm opt} = \sqrt{(I_{\rm rms}^2 R_{\rm dson})/(E_{\rm switch} f)} \times A_{\rm ref}$ where $I_{\rm rms}$ is the root-mean-square (rms) current [7], $R_{\rm dson}$ is the resistance of the drain-source channel of $M_{\rm ref}$, and $E_{\rm switch}$ represents the energy loss associated with the parasitic capacitance of the junctions formed by drain, source, and gate of $M_{\rm ref}$. $R_{\rm dson}$, and $E_{\rm switch}$ were found through simulations using commercial circuit simulation software (PSPICE) and are listed in Table I.

The efficiency and power density of the converter are calculated to complete the inductor design process for a given ripple ratio and frequency. This process is repeated for different combinations of ripple ratio and frequency, and the results giving the best power density for a given efficiency are plotted. The results of the loss calculations were compared with measured results on V-groove inductors with a $Co\text{-}ZrO_2$ core in [4].

III. MATERIALS

Using the design process described in Section II we proceed to investigate the performance of a 3.3- to 1.1-V, 7-A dc-to-dc converter, using different materials as the core in the V-groove inductor. We start by considering Co-Zr-O films. Ohnuma *et al.* [8] have deposited these films with different atomic compositions and measured the resulting magnetic properties. For several of these materials, listed in Table II, we analyzed and plotted, in Fig. 2, the predicted performance of the converter using an inductor based on these films. A maximum power dissipation curve shown in Figs. 2–4, is based on the maximum power dissipation limit of 500 watts/cm^2 in typical power semiconductor devices [9].

We can use Fig. 2 to establish which composition is preferred for any given region of power density and efficiency. For example, composition 3 ($Co_{63.5}Zr_{10}O_{26.5}$) gives the largest power density (>1120 W/cm^2) for efficiencies below 84%, and com-

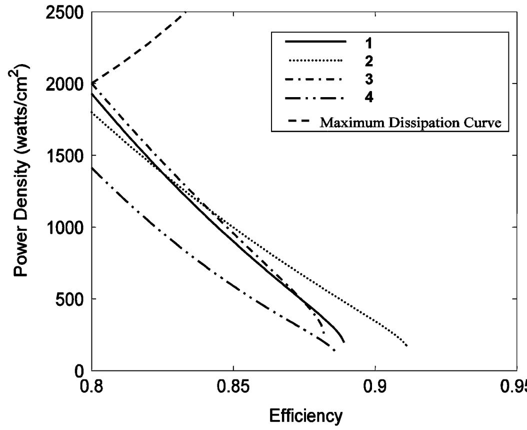

Fig. 2. Power density versus efficiency plot for converters using V-groove inductors based using Co-Zr-O films. The Y axis represents the power output per substrate area including the area used by the inductor and the MOSFETs. The X axis represents the efficiency taking into account the losses in the inductor and the MOSFETs. The dotted line represents a maximum power dissipation curve as discussed in the text. The numbers in the legend correspond to the material compositions listed in Table II.

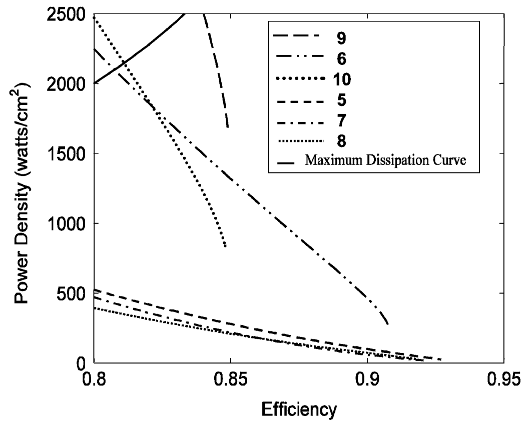

Fig. 3. Power density versus efficiency plot showing converter performance similar to Fig. 2, but using inductors based upon: Fe-Al-O and Co-Fe-B-Si-O films. The numbers in the legend refer to the compositions in Table III.

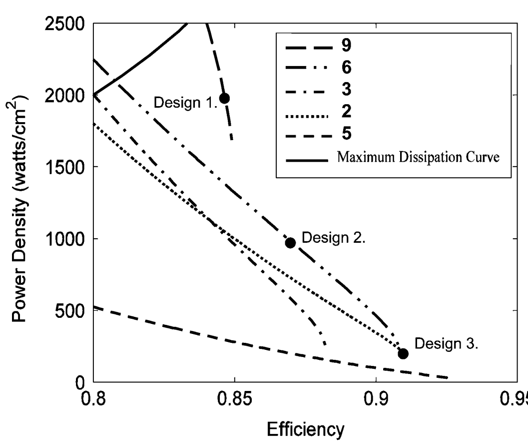

Fig. 4. Power density versus efficiency curves, similar to Fig. 2 for the best converter performance using the three materials investigated: Co-Zr-O, Fe-Al-O, and Co-Fe-B-Si-O. The numbers in the legend refer to the materials in Tables II and III. Designs 1, 2, and 3 refer to three different converter designs mentioned in Table IV.

TABLE III
PROPERTIES OF Fe-Al-O [1], [10] AND Co-Fe-B-Si-O [11] FILMS

No.	*Composition*	B_s (T)	H_c (Oe)	ρ ($\mu\Omega$-cm)	μ_r
5	$Fe_{61}Al_{13}O_{26}$	1.2	1	800	300
6	$Fe_{70}Al_{11}O_{19}$	1.6	1	300	100
7	$Fe_{48}Al_{18}O_{34}$	0.9	1	2800	290
8	$(Co_{66.6}Fe_{6.4}B_{26})_{0.9}(SiO_{1.9})_{0.1}$	0.68	1	400	140
9	$(Co_{36.5}Fe_{50}B_{14.4})_{0.74}(SiO_{1.9})_{0.26}$	1.06	1	107,000	25
10	$Co_{38.5}Fe_{4.7}B_{14.5}$	1.76	1	100	50

TABLE IV
CONVERTER DESIGNS USING THE THREE DIFFERENT MATERIALS

Design	Material	Power Density (W/cm^2)	Efficiency (%)	Ripple Ratio	Frequency (MHz)
1	9	2000	85	1.9	65
2	6	975	87	0.8	43
3	2	250	91	1.2	16

position 2 ($Co_{64}Zr_{10}O_{26}$) gives the largest power density for efficiencies above 84%.

The compositions in Table II were picked after several iterations of optimization. A number of films with similar composition were grouped into clusters. The compositions selected for inclusion in Table II were those that had the best overall power density vs efficiency performance in their respective clusters.

From Fig. 2 we can see the best performance achievable with Co-Zr-O, and can identify appropriate compositions for different efficiencies and power densities. We now undertake a similar comparison using two other candidates materials. We pick two compositions that have high M_s and high resistivity: Fe-Al-O [1], [10], and Co-Fe-B-Si-O [11]. The data in Table III is obtained from [1], [10], [11]. As the coercivity values for these films were unavailable, they were assumed to be 1 Oe.

Fig. 3 shows the power density versus efficiency curves for materials in Table II. We can eliminate some of these compositions (7, 8, and 10) as candidates for use as core material. For example, for high efficiencies, at lower power density, one would choose composition 5 over 7 and 8. Similarly, at higher power densities, either compositions 6 or 9 would be chosen over 10.

Finally, a comparison of best curves from Figs. 2 and 3 is made in Fig. 4. Composition 6 ($Fe_{70}Al_{11}O_{19}$) gives the highest power density for efficiencies from 81% to 91%. Composition 2 ($Co_{64}Zr_{10}O_{26}$) gives a similar performance for most efficiencies, and is capable of slightly higher efficiencies at low power densities (<250 W/cm^2). Similarly, composition 5 ($Fe_{61}Al_{13}O_{26}$), can achieve even higher efficiencies (up to 93%) at very low power densities of 25 W/cm^2 and below. Composition 9 [$(Co_{36.5}Fe_{50}B_{14.4})_{0.74}(SiO_{1.9})_{0.26}$] gives the highest power density at low (<85%) efficiencies, but these designs rapidly approach the power density limit and so are unlikely to be of much practical value.

Three different converter designs using the three inductor core materials investigated above are listed in Table IV. To obtain the desired power density and efficiency characteristics of the converter, one must operate the devices at the given ripple ratio and the frequency, using the respective materials as the core in the inductor.

Higher resistivity and higher M_s always improve performance but resistivity is more important for high-efficiency, low-power-density designs, whereas M_s is more important for high-power-density, lower-efficiency designs. The ideal permeability depends on the design objectives. For high power density at lower efficiencies, lower permeability is best (e.g., $\mu_r = 25$ for composition 9). However, for high efficiency at lower power density, higher permeability is best (e.g., $\mu_r = 300$ for composition 5).

IV. CONCLUSION

In order to evaluate candidate soft magnetic materials for use in thin-film inductors for microfabricated dc-to-dc converters, we have developed an optimization routine which evaluates the achievable efficiency and power density of the converter using designs individually optimized to make best use of particular materials. The optimization selects switching frequency, ripple ratio, inductor dimensions and MOSFET sizes.

For the example application of a 3.3- to 1.1-V, 7-A output converter, Co-Zr-O, Fe-Al-O, and Co-Fe-B-Si-O materials have been evaluated. For most applications, we have identified $Fe_{70}Al_{11}O_{19}$ and $Co_{64}Zr_{10}O_{26}$ as the best candidates, with similar performance. $Fe_{70}Al_{11}O_{19}$ is better for lower efficiencies and higher power density applications and $Co_{64}Zr_{10}O_{26}$ is better in a few higher efficiency, lower power density applications. The final choice of material will also depend on practical considerations involving ease of deposition, reliability, and material compatibility.

The methodology introduced here will also help guide development and evaluation of new materials.

REFERENCES

[1] Y. Shimada, M. Yamaguchi, S. Ohnuma, T. Itoh, W. Li, S. I. Ans, K. H. Kim, and H. Nagura, "Granular films with high permeability," *IEEE Trans. Magn.*, vol. 39, pp. 3052–3056, May 2003.

[2] G. I. Mehas, K. D. Coonley, and C. R. Sullivan, "Converter and inductor design for fast-response microprocessor power delivery," *APESC*, pp. 1621–1626, June 2000.

[3] S. Prabhakaran, C. R. Sullivan, and C. G. Levey, "Fabrication of thin-film V-groove inductors using composite magnetic materials," in *Proc. IMAPS Advanced Technology Workshop Integrated Power Passives Integration*, Ogunquit, ME, June 2002.

[4] S. Prabhakaran, C. R. Sullivan, and K. Venkatachalam, "Measured electrical performance of V-groove inductors for microprocessor power delivery," *IEEE Trans. Magn.*, vol. 39, pp. 3190–3192, May 2003.

[5] Predictive Technology Model (2003). [Online]. Available: http://www-device.eecs.berkeley.edu/~ptm/

[6] L. C. Hu, *Silicon and Beyond—Advanced Device Models and Circuit Simulators*. Singapore: World Scientific, 2000, ch. 1, pp. 1–31.

[7] R. W. Erickson and D. Maksimovic, *Fundamentals of Power Electronics*, 2nd ed. Norwell, MA: Kluwer Academic, 2001.

[8] S. Ohnuma, H. Lee, N. Kobayashi, H. Fujimori, and T. Masumoto, "Co-Zr-O nano-granular thin films with improved high frequency soft magnetic properties," *IEEE Trans. Magn.*, vol. 37, p. 2251, July 2001.

[9] C. Sullivan and S. Sanders, "Design of microfabricated transformers and inductors for high-frequency power conversion," *IEEE Trans. Power Electron.*, vol. 11, pp. 228–238, Mar. 1996.

[10] W. D. Li, "Magnetic anisotropy and dynamic properties of highly resisitive soft granular films," Ph.D. thesis, Tohuku Univ., Sendai, Japan, 1998.

[11] M. Munakata, M. Namikawa, M. Motoyama, M. Yagi, Y. Shimada, M. Yamaguchi, and K. Arai, "Magnetic properties and frequency characteristics of $(CoFeB)_x(SiO_{1.9})_{1-x}$ and CoFeB films for RF application," *Trans. Magn. Soc. Japan*, vol. 2, p. 388, 2002.